Food web complexity alters phytoplankton persistence and resilience to nutrient pulses in experimental ecosystems

Tyler J. Butts[1,2*], Robert A. Johnson[1,3], Michael J. Weber[4], Grace M. Wilkinson[1,2,3]

[1]Department of Ecology, Evolution, and Organismal Biology, Iowa State University, Ames, IA, USA

[2]Present Address: Center for Limnology, University of Wisconsin-Madison, WI, USA

[3]Present Address: Department of Integrative Biology, University of Wisconsin-Madison, Madison, WI, USA

[4]Department of Natural Resource Ecology and Management, Iowa State University, Ames, IA, USA

* Corresponding author: Tyler J. Butts, email: tjbutts@wisc.edu

Open research statement: Data is archived at the Environmental Data Initiative (https://doi.org/10.6073/pasta/c5b157a1b0f294404627494dfc1587e7) and scripts are archived through Zenodo (https://doi.org/10.5281/zenodo.18133475)

A peer-reviewed and edited version of this manuscript has been accepted at *Limnology & Oceanography* as an open-access publication. This pre-print represents an older version of the manuscript, the updated version differs slightly in content and terminology following the peer-review process. The final version of this manuscript is available via the 'peer-reviewed publication DOI' link on the right-hand side of this webpage. Please feel free to contact the corresponding author and please only cite and review the *Limnology & Oceanography* publication as that is the most accurate and final manuscript.

Keywords/phrases: pulse perturbation; benthic-pelagic coupling; resistance; resilience; food web structure; phytoplankton; shallow lakes; experimental ponds

ABSTRACT

Food webs may mediate the resistance and resilience of ecosystems to disturbances driven by climate change. In aquatic ecosystems, greater food web complexity is theorized to increasing the resistance (longer response time) and resilience (shorter recovery time) of primary production to pulse disturbances, yet experimental evidence is limited. We simulated two storm-induced pulse disturbances by adding nutrients (~3%, ~5% increase in ambient concentrations) to three ponds with low, intermediate, and high food web complexity and compared them to reference ponds with matching food web structures. We evaluated primary production response time (resistance) and recovery time (resilience) following each nutrient pulse using a response detection algorithm and evaluated evidence of a critical transition with online dynamic linear modeling (resilience). The response threshold was never exceeded in the high complexity pond following either nutrient pulse whereas the threshold was exceeded in both the intermediate and low complexity ponds following the first pulse. There was evidence of a critical transition in the low complexity pond following the first pulse. After the second nutrient pulse, chlorophyll-*a* exceeded the response threshold again in both low and intermediate ponds, but the response was 12 days faster and the recovery 14 days longer in the low complexity pond. The intermediate pond was on track for a faster recovery time before the end of the experiment. We empirically show that greater food web complexity confers greater resistance and resilience of phytoplankton to repeated pulses of nutrient loading and may help buffer aquatic ecosystems against increasing and intensifying disturbances.

INTRODUCTION

The frequency, scale, and intensity of disturbances are increasing with accelerating climate change (Seneviratne et al. 2021). Changes to disturbance regimes are also increasing the likelihood of abrupt change, rapid shifts in ecosystem state relative to typical rates of change within the ecosystem (Turner et al. 2020). For example, extreme heat waves have been linked to mass bleaching events in coral reefs (Hughes et al. 2018) while extreme precipitation, coupled with agricultural land use, has been tied to increased eutrophication and higher abundances of phytoplankton in aquatic ecosystems (Ho and Michalak 2020). Disturbances can alter ecosystem function and dynamics, and changing environmental drivers and disturbance regimes may interact in novel ways affecting ecosystem response (Zscheischler et al. 2018). Understanding the mechanisms mediating effects of disturbance on ecosystem function is imperative for effective ecosystem management in the face of global change.

Pulse disturbances, sudden and temporally constrained disturbances that alter biomass or composition of ecological communities, are ubiquitous in ecosystems and expected to increase in number and severity (Prein et al. 2017). In many lakes, annual nutrient loading is dominated by a few loading events during large storms (Carpenter et al., 2018; Joosse & Baker, 2011). Eutrophication leads to higher turbidity, depleted dissolved oxygen (DO), and proliferation of toxin-producing phytoplankton that adversely affect human health (Carmichael and Boyer 2016). Not all lakes respond to nutrient pulses in the same way as antecedent conditions, ecosystem properties, and watershed characteristics affect whether nutrients from storms will alter ecosystem function or trigger an abrupt change (Stockwell et al. 2020). Thus, there is a pressing need to better understand mechanisms that mediate aquatic ecosystem responses to pulse nutrient disturbances.

The architecture of food web interactions plays a critical role in determining aquatic ecosystem function and dynamics in response to increasing and interacting disturbances (Rooney and McCann 2012; Wootton and Stouffer 2016). Food webs can influence ecological stability through their trophic structure and connectivity affecting resistance and resilience (Wojcik et al. 2021). Here, resistance is defined as the maximum temporary change in a variable that describes the ecosystem state following a pulse disturbance, and resilience is defined as the rate of return in that variable following a disturbance, which is slower closer to a critical transition (Cottingham and Schindler 2000; Taranu et al. 2018). For example, in a whole-ecosystem nutrient pulse experiment in two small lakes, alterations to food chain length through the addition of a planktivore led to decreased ecosystem resistance to nutrient pulses (Cottingham and Schindler 2000). Food web structure can also be characterized within-trophic levels corresponding to the degree of resource coupling between food chains (Vadeboncoeur et al. 2005; Ward et al. 2015) or the number of species present within a trophic level (Duffy et al. 2007). Put together, both food chain length and within-trophic level connectivity and richness increases food web complexity and may affect resistance and resilience to pulse disturbances.

Food web complexity can influence resistance and resilience to pulse disturbances through multiple and simultaneously acting mechanisms (Duffy et al. 2007). Even-numbered food chains can strengthen top-down control on primary producers (Carpenter et al., 2001; Pace et al., 1999). Stronger top-down control may reduce the amplitude of biomass oscillations of primary producers in response to a sudden influx of nutrients. A greater degree of resource coupling between food chains, such as phytoplankton-based and periphyton/detritus-based food chains, can provide higher resource subsidies to consumers (Vadeboncoeur et al. 2005) as well as increase food web connectivity generating more pathways for nutrients to flow and greater resource use efficiency within food webs (Rooney and McCann 2012; Ceulemans et al. 2019). As a result, an even-number of trophic levels, greater species diversity within trophic levels, and higher connectivity should increase resistance and resilience of primary producer biomass to nutrient pulse disturbances. While several recent models have indicated greater food web complexity increases the resistance and resilience of ecosystems to disturbances (Wojcik et al. 2021; Adje et al. 2023; Polazzo et al. 2023), they often are built with only one or two trophic levels and only evaluate a single disturbance. Consequently, there remains a need to demonstrate empirically how, and to what extent, food web complexity modulates resistance and resilience to multiple pulse disturbances.

We performed a set of whole-ecosystem manipulations to empirically evaluate if greater food web complexity affects ecosystem response to pulse nutrient loading events. Specifically, we asked (1) does a higher degree of food web complexity affect the magnitude of response of primary production to nutrient pulses? and (2) does a higher degree of food web complexity influence the resistance and resilience of primary producer biomass to nutrient pulses? We predicted greater food web complexity would result in slower response times and a low magnitude of response in primary production to nutrient pulses (i.e., greater resistance) and faster recovery times to baseline conditions (i.e., greater resilience). We also predicted a higher degree of food web complexity would reduce the chance of an abrupt change in primary production due to greater resilience to nutrient pulse disturbances.

METHODS

The experiment occurred in summer 2020 at the Iowa State Horticultural Research Station (42.110005, -93.580454) in six experimental ponds (surface area = 400 m^2, maximum depth = 2m). The catchments are limited to a few meters on each side and the bottom sealed with bentonite clay. The only hydrologic input was direct precipitation. In April 2020, the ponds were filled with water from the on-site irrigation reservoir seeding each pond with a similar assemblage of phytoplankton and zooplankton. Emergent longleaf pondweed (*Potamogeton nodosus*) and submerged leafy pondweed (*Potamogeton foliosus*) were naturally established in each pond.

Experimental Design

We established three fish assemblages with low, intermediate, and high food web complexity (Figure 1). We varied food chain length and within-trophic level species richness to better differentiate responses due to food web complexity. For example, if the number of trophic levels was the main driver of ecosystem response, we would not expect to see a difference in ponds with the same number of trophic levels. Instead, we could attribute a difference in response to other aspects of food web structure such as species richness within trophic levels. We randomly assigned each fish assemblage to two ponds, one receiving the nutrient pulses and one serving as an unmanipulated reference. The treatments were not replicated due to the availability of experimental ponds, but the comparison of a manipulated to reference ecosystem is a common study design for whole-ecosystem manipulations (Carpenter 1998). Moreover, the large-scale experiment we performed reduces potentially misleading inferences by assessing food web complexity at the scale in which ecological processes are occurring (Carpenter 1996; Schindler 1998).

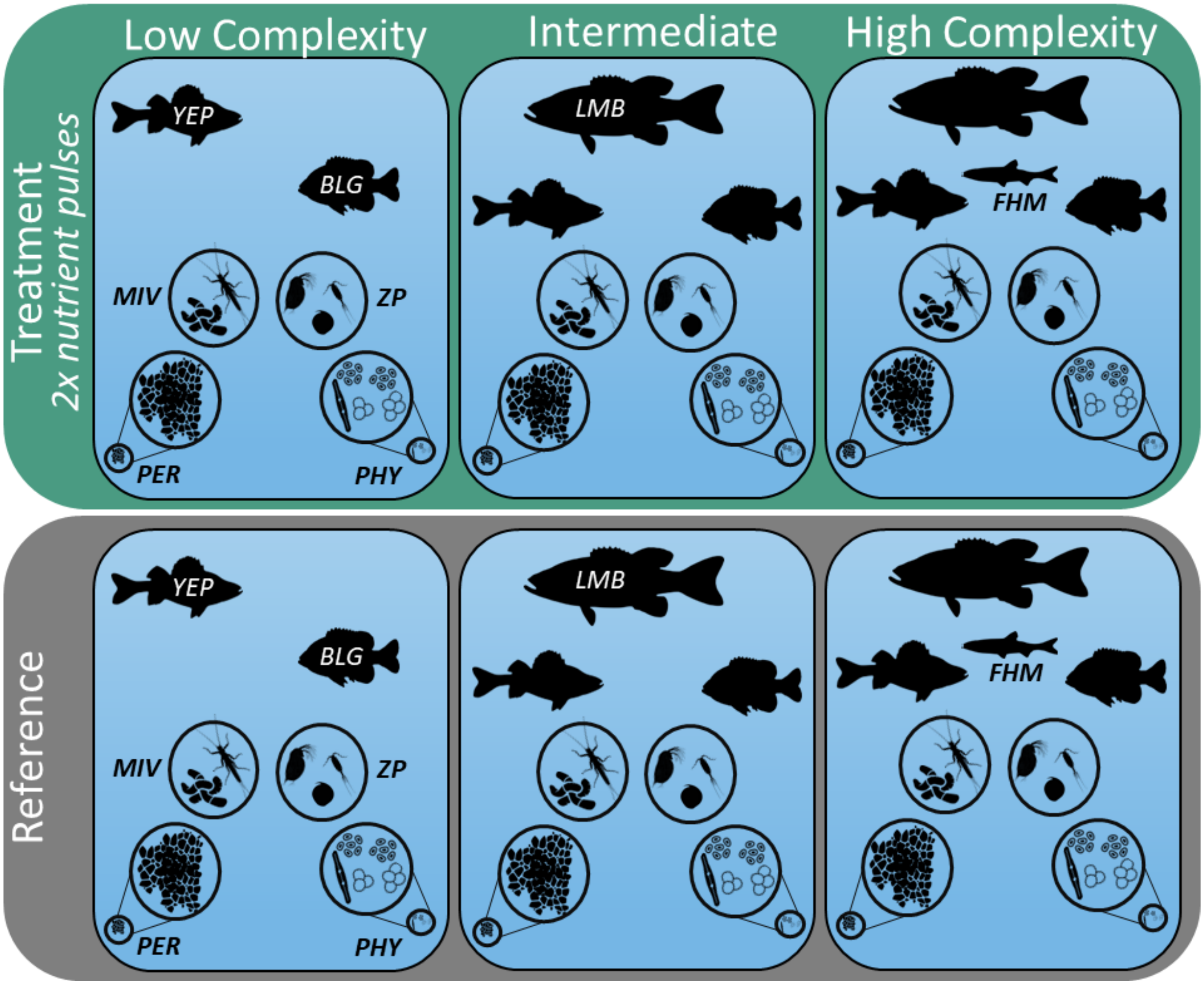

Figure 1. Diagram of food web structures in the ponds. Structures were duplicated and randomly assigned; one duplicate received the nutrient pulse while the other served as the unmanipulated reference. Taxa are periphyton (PER), phytoplankton (PHY), macroinvertebrates (MIV), zooplankton (ZP), yellow perch (YP), bluegill (BG), largemouth bass (LMB), and fathead minnows (FHM).

We inferred trophic connections based on literature descriptions and fish diet samples (Supplementary Material). The ponds with the lowest food web complexity (hereafter, low complexity) consisted of three trophic levels and two food chains. The first food chain included planktivorous bluegill (*Lepomis macrochirus,* Werner and Hall 1988), zooplankton, and phytoplankton, and the second included zoobenthivorous yellow perch (*Perca flavescens*, Tyson and Knight 2001), macroinvertebrates, and periphyton and detritus. Food web complexity was increased in the next assemblage (hereafter, intermediate complexity) by adding a fourth trophic level containing a generalist consumer, largemouth bass (*Micropterus salmoides*), that preys across food chains and trophic levels (i.e., omnivory; (Hodgson and Hodgson 2000). Although ecosystem size constrains food chain length (Post et al. 2000; Pomeranz et al. 2023), the top predator in our system, largemouth bass, commonly inhabit similar size ponds in the region (Guy and Willis 1990). Finally, we again increased food web complexity (hereafter, high complexity) through the addition of fathead minnows (*Pimephales promelas*, Duffy 1998), a generalist consumer at the third trophic level.

Fish biomass for each species was kept consistent amongst ponds (Table 1). With additional fish species, we held the species biomass consistent amongst ponds; therefore, total fish biomass increased. We chose an additive design to preserve natural complexity, assess how the ecosystem adapted and stabilized over time, and focus on interactions between species rather than confound intra- and interspecific interactions which can occur with a substitutive design (Griffen 2006; Carey and Wahl 2010). Total fish biomass for all ponds (40 – 80 kilograms per hectare, kg ha^{-1}) fell within the range of values reported (28 – 305 kg ha^{-1}) for several North American lakes (Carlander 1977). Fish were collected with electrofishing from nearby Brushy Creek Lake (42.39194, -93.98917) and Five Island Lake (43.15806, -94.64667). Fathead minnows were purchased from Beemer Fisheries in Bedford, IA.

Table 1. Mean (s.d.) of water quality metrics (n=46 – 47) and fish biomass (n.p. = not present). Pulsed refers to ponds that received the two nutrient additions and reference are unmanipulated ponds.

	Low complexity		**Intermediate**		**High complexity**	
Variable	***Pulsed***	***Reference***	***Pulsed***	***Reference***	***Pulsed***	***Reference***
Total P (μg L^{-1})	39 (11)	47 (22)	70 (47)	51 (36)	35 (12)	46 (12)
Total N (mg L^{-1})	0.39 (0.15)	0.41 (0.15)	0.41 (0.20)	0.42 (0.18)	0.39 (0.16)	0.36 (0.15)
Soluble P (μg L^{-1})	3.9 (0)	4.2 (0.94)	4.0 (0.30)	5.3 (2.5)	3.9 (0)	7.2 (5.2)
Nitrate – N (mg L^{-1})	0.13 (0.070)	0.12 (0.070)	0.13 (0.082)	0.14 (0.077)	0.13 (0.073)	0.13 (0.081)
Ammonium – N (mg L^{-1})	0.024 (0.023)	0.022 (0.027)	0.016 (0.019)	0.013 (0.017)	0.015 (0.016)	0.024 (0.029)
Bluegill (kg ha^{-1})	21	20	21	21	20	21
Yellow Perch (kg ha^{-1})	20	20	20	19	19	20
Largemouth Bass (kg ha^{-1})	n.p.	n.p.	24	26	23	30
Fathead Minnow (kg ha^{-1})	n.p.	n.p.	n.p.	n.p.	9.0	9.0

Yellow perch were stocked on day of year (DOY) 98- 99 with additional perch added on DOY 127 to replace individuals that died from stress or natural mortality. We added bluegill on DOY 127,128, and 133. On DOY 141, we added largemouth bass to both the intermediate and high complexity ponds, and fathead minnows only to the high complexity ponds. There was a small population of remnant bigmouth buffalo (*Ictiobus cyprinellus,* age-1) in the pulsed low complexity pond (n=10) and reference high complexity pond (n=2) from an ecosystem experiment the previous year that were not detected until the end of the experiment. While bigmouth buffalo likely contributed to increased zooplanktivory within the ponds, they are not generalist consumers (Starostka and Applegate 1970, Adámek et al. 2003) and did not confound the intended degrees of complexity present within our food web configurations.

We performed two discrete nutrient additions (i.e., pulses) to three of the ponds, one from each food web treatment, on DOY 176 and DOY 211 (Figure 1). Ambient nutrients were similar amongst the ponds though P was slightly elevated in the reference ponds compared to the pulsed ponds (Table 1). We designed the nutrient pulses to simulate the magnitude and stoichiometry of storm-driven nutrient loading in an agricultural catchments (Vanni et al. 2001; Lürling et al. 2018). The pond volume (~450 m^3) and nutrient concentrations measured the week prior to the nutrient pulses were used to determine the mass of nitrogen (N) and phosphorus (P) to add (Supplementary Material Table S1) such that the first and second pulses resulted in a 3% and 5% increase in P concentration, respectively. Ammonium nitrate (NH_4NO_3) and sodium phosphate monobasic dihydrate ($NaH_2PO4•H_2O$) at a 24N:1P ratio were dissolved in a 4 L carboy of water taken from the pond and slowly dispensed by kayak across the surface of the pond over 30 minutes. Two meteorological disturbances occurred during the experiment. The first was a six-day period of elevated surface water temperatures that occurred nine days after the first nutrient pulse (DOY 185 – 190) and the second was a derecho on DOY 223 after the second nutrient pulse. Neither disturbance increased nutrient loading to the ponds due to the lack of a catchment.

Data Collection

Daily data collection began on DOY 142, 34 days prior to the first nutrient addition. We collected water samples three times per week from 0.25 m depth to measure total and dissolved nutrients. For dissolved nutrients, samples were filtered in the field through Whatman glass fiber filters (0.45 µm); whole water samples were used for total nutrient analysis. Samples were kept on ice until transport to the lab and preserved with 100 µL of concentrated sulfuric acid (Supplementary Material). To assess the response of primary production to the nutrient pulses, we measured chlorophyll-*a* concentration, a proxy for phytoplankton biomass using a Total Algae Sensor on a YSI Handheld sonde (Xylem, Yellow Springs, Ohio, USA). The mean chlorophyll-*a* value from 0.1-0.3 m depth was used in the statistical analyses. As phytoplankton were not the only primary producers in the ponds, we also measured ecosystem metabolism using dissolved oxygen (DO) concentrations measured every 30 minutes using miniDOT loggers (Precision Measurement Engineering, Vista, California, USA) deployed at 0.25 m over the deepest point to quantify the response of all primary producers to the nutrient additions. An on-site weather station (Onset HOBO U30 USB) provided measurements of photosynthetic active radiation and wind speed.

Daily rates of gross primary production (GPP), ecosystem respiration (R), and net ecosystem production (NEP) were estimated using the Kalman filter method in the *LakeMetabolizer* package in R (Winslow et al. 2016). Prior to analysis, DO data were cleaned by removing measurements where DO decreased by more than 2.0 mg L^{-1} from the previous measurement and the subsequent five DO measurements. These sharp declines coincided with water column mixing, erroneously influencing metabolism estimates. Data gaps were filled through linear interpolation. Metabolic rates calculated from free-water oxygen measurements can result in erroneous estimates (i.e., negative GPP, positive R) when physical processes have a stronger effect on DO than biological processes (Rose et al. 2014). Erroneous metabolism estimates (4-18% of days depending on the pond) were removed prior to statistical analysis.

We also monitored biomass of periphyton, zooplankton, macroinvertebrates, and fish gut content. Periphyton areal biomass was estimated biweekly using modified Hester-Dendy samplers. Zooplankton were sampled twice per week via a 1 m vertical tow of a Wisconsin net (63 µm mesh). Zooplankton crustaceans and rotifers were identified to genus, excluding copepods identified to order, and length-mass regressions were used to calculate biomass (Dumont et al. 1975; McCauley 1984). Macroinvertebrates were sampled biweekly using a modified stovepipe sampler (Jackson et al. 2019) and identified to family (mollusks and insects) or class (leeches and oligochaetes) using a stereomicroscope. At the end of the experiment, fish (except for fathead minnows) stomach contents were retrieved through gastric lavage and identified to the lowest possible taxonomic order using a stereomicroscope. Additional details of sample collection and analysis are in Supplementary Material.

Data Analysis

We used the response detection algorithm (Walter et al. 2022) in the *disturbhf* package in R (Walter and Buelo 2022) to quantify the response and recovery time of chlorophyll-*a* and ecosystem metabolism (state variables) to nutrient pulses in each food web complexity treatment. The algorithm calculates the empirical cumulative distribution function (ECDF) for each rolling window of the state variable in the disturbed ecosystem (i.e., nutrient addition pond) and compares it to the ECDF calculated for the entirety of the state variable time series in the reference ecosystem. The maximum difference in the ECDF for each rolling window of the disturbed pond time series is compared to the reference ECDF and expressed as a time series of Z-scores. The Z-score quantifies the difference in ECDFs between the disturbed and reference time series to the mean of the reference ECDF, expressed as standard deviation. We used the entire reference time series rather than an adaptive window to compare the response of the disturbed ecosystem to the total variability expected without any nutrient pulses. We chose a rolling window of seven days to capture rapid changes in primary production following each nutrient pulse. We performed sensitivity analyses using five- and ten-day rolling windows and found minimal differences (Supplementary Material: Table S4). Following Walter et al. (2022), we defined the response time (i.e., resistance) to the nutrient pulses as the number of days after the addition until the Z-score exceeded 2.0. This threshold indicates a significant and rare event that is a substantial departure from reference conditions. Recovery time (i.e., resilience) was defined as the number of days for the Z-score to return to <0.5 following a significant response (Z-score > 2.0). This recovery time threshold indicates a return to reference conditions in the disturbed ecosystem.

We used online dynamic linear modeling to detect if the pulsed ponds approached or crossed a threshold (i.e., critical transition) from a low to high chlorophyll-*a* concentration state as a measure of resilience (Taranu et al. 2018). Critical transitions are defined as an unstable equilibrium point where the rate of return to equilibrium approaches zero and the disturbance regime brings the boundary between two basins of attraction closer together (Guttal and Jayaprakash 2008; Scheffer et al. 2015). This is indicative of a critical slowing down where the system recovers more slowly to perturbations (Dakos et al. 2012; Scheffer et al. 2015). Changes in indicators of resilience are qualitatively indicative of the ecosystem gaining or losing resilience. The online dynamic linear modeling method requires a complete daily time series and therefore could not be applied to the metabolism estimates. Briefly, this method calculates the eigenvalues of a time series by fitting autoregressive models (AR) with time-varying coefficients. When the eigenvalues of a state variable increase to be greater than one it is indicative that the state variable is no longer rapidly returning towards the mean as calculated by the autoregressive model of sequential rolling windows of observation (Dakos et al. 2012). This is taken as evidence that the system crossed a critical threshold but does not necessarily indicate a permanent regime shift has occurred. We fit time-varying AR (p) models to chlorophyll-*a* for each pond with an optimal order of one or two with model selection using Akaike's Information Criteria corrected for small sample size (AICc; Hurvich & Tsai, 1993; Supplementary Material Table S2). All analyses were performed in R version 4.2.1 (R Core Team 2022).

RESULTS

The food web structures established within the ponds led to different food web dynamics (Figure 2). Initially, zooplankton biomass was similar amongst ponds but diverged after a few weeks (Figure 2A - C). Zooplankton biomass in the low complexity ponds steadily decreased (Figure 2A), resulting in the lowest mean biomass in this treatment (Supplementary Material Figure S1A). In the intermediate and high complexity ponds, zooplankton biomass only modestly declined (Figure 2A - C), resulting in higher mean biomass (Supplementary Material Figure S1B - C). Macroinvertebrate density was variable (Figure 2D - F), with the highest densities in the high complexity pond (Figure 2F, Supplementary Material Figure S1D - F).

Periphyton areal biomass was low in the low complexity ponds, but steadily increased in the pulsed low complexity pond and all reference ponds (Figure 2G - I, Supplementary Material Figure S1G - I). Fish diets collected at the end of the experiment roughly corresponded to our expectations of trophic interactions with bluegill mainly preying on zooplankton and yellow perch consuming a greater abundance of macroinvertebrates (Supplementary Material Table S3). Largemouth bass preyed on a diversity of organisms, but mostly fish and macroinvertebrates (Supplementary Material Table S3). The nutrient pulses effectively increased ambient nutrient concentrations in the pulsed ponds; there was an increase in nutrient concentrations following each pulse in comparison to concentrations prior to the addition (Supplementary Material Figure S2).

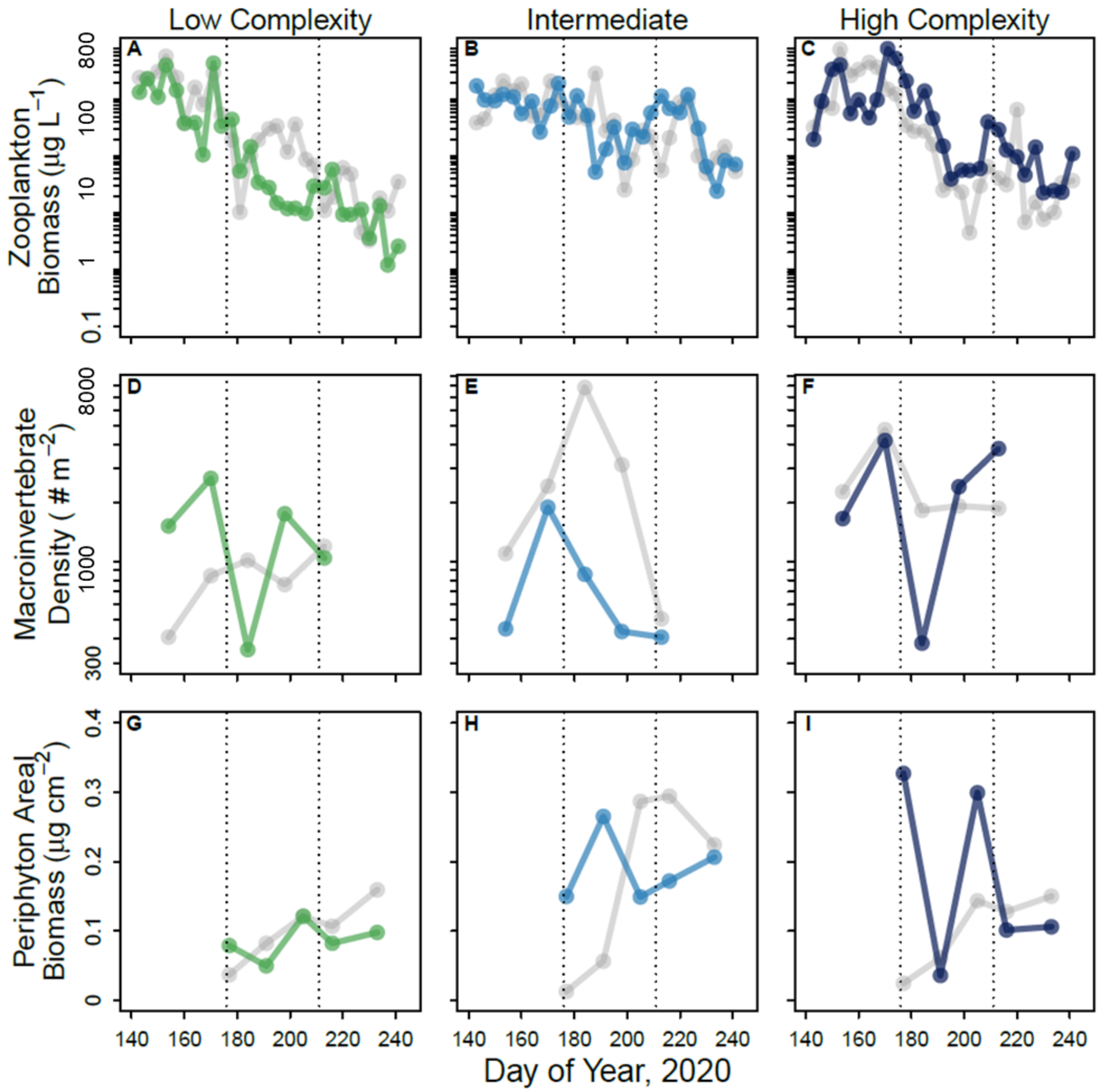

Figure 2. Time series of zooplankton biomass (A-C), macroinvertebrate density (D - F), and periphyton areal biomass (G - I). The darker line is the disturbed time series, the gray line is the reference time series.

Following the first nutrient pulse, chlorophyll-*a* concentrations increased and peaked at roughly the same time in both the low (DOY 198) and intermediate (DOY 194) complexity ponds (Figure 3A - B). In comparison, there was no response of chlorophyll-*a* in the high complexity pulsed pond (Figure 3C). Following the second nutrient pulse, chlorophyll-*a* concentration increased in all three pulsed ponds with the low complexity pond peaking first on DOY 224, the intermediate complexity on DOY 232, and the high complexity pond on DOY 236. Gross primary production (GPP), which encompasses production from all primary producers, was similar to the chlorophyll-*a* dynamics after both nutrient pulses in the intermediate and high complexity ponds but dissimilar in the low complexity pulsed pond (Figure 3D - F). Respiration (R) steadily increased for all pulsed ponds over the duration of the experiment and followed the reference ponds closely (Figure 3G - I). Net ecosystem production (NEP) initially decreased then remained largely heterotrophic for all ponds following the first nutrient pulse (Figure 3J - L). There was an increase in NEP following the first nutrient pulse in the intermediate complexity pulsed pond akin to the dynamics observed in gross primary production and chlorophyll-*a* (Figure 3H). However, the reference intermediate complexity pond had similar dynamics. The low and intermediate complexity ponds became heterotrophic prior to the first nutrient pulse (between DOY 151 - 172) and remained heterotrophic until the end of the experiment (Figure 3J - K). Both the pulsed and reference high complexity ponds remained autotrophic longer than the other two food web structures, becoming heterotrophic on DOY 192 (Figure 3L).

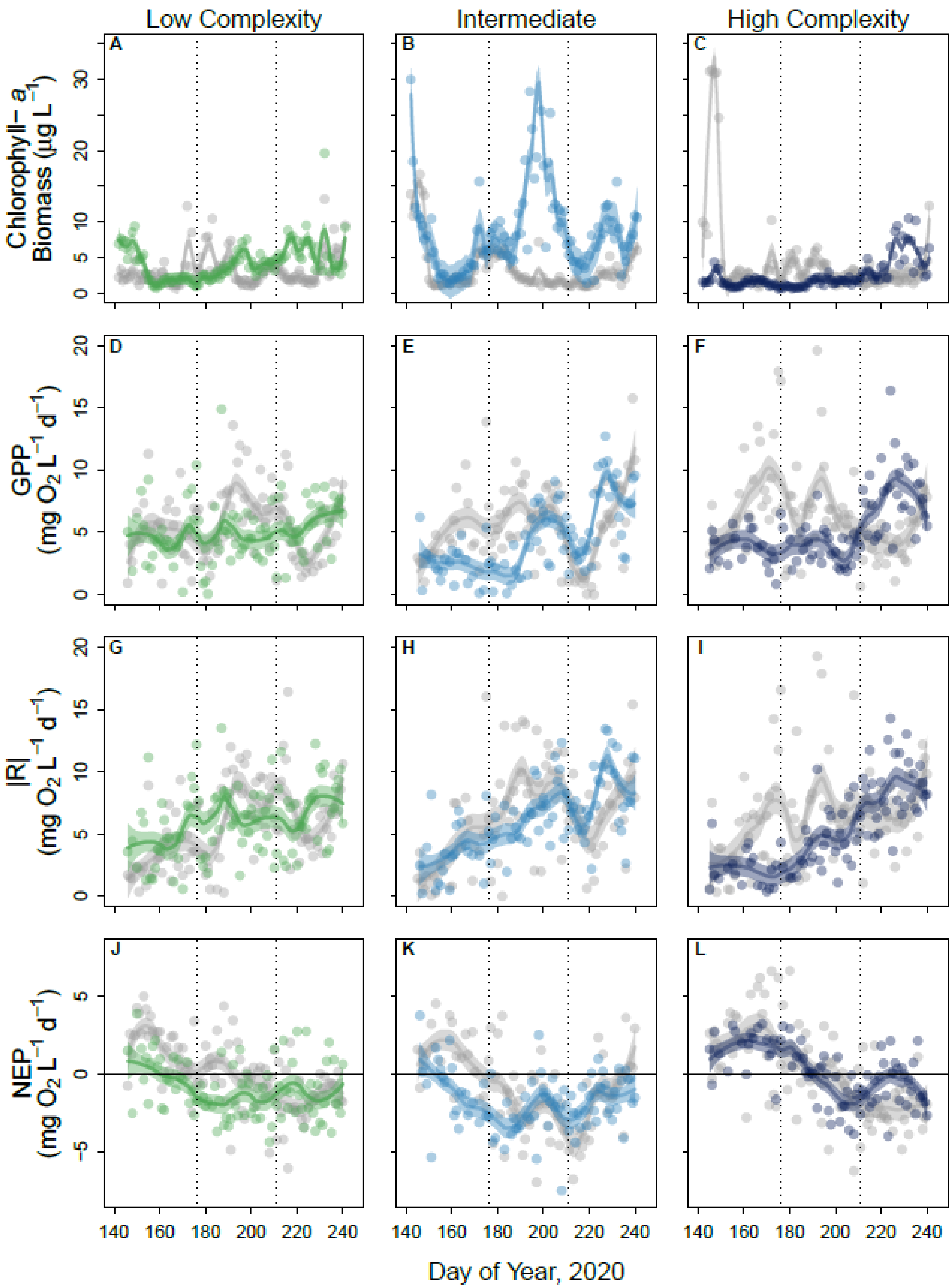

Figure 3. Dynamics of chlorophyll-*a* (A - C), gross primary production (GPP, D - F), respiration (absolute value, |R|, G - I), and net ecosystem production (NEP, J - L). Data were fitted with

LOESS regression analysis (10% span) for visualization, the shaded region is standard error. The dark line is the disturbed pond, and the dark gray line is the reference pond. The dashed vertical line denotes the nutrient pulses and the horizontal line at zero (J - L) denotes autotrophic (NEP > 0) or heterotrophic (NEP < 0) conditions.

We found support for our prediction that the resistance and resilience of primary production to the nutrient pulses would be greatest in the high complexity pond (Figure 4). Following the first nutrient pulse, chlorophyll-*a* Z-scores for the low and intermediate complexity ponds surpassed 2, indicating a significant response, whereas there was no significant response detected in the high complexity ponds (Figure 4A - B). There was a significant recovery (Z-score decreased below 0.5) prior to the second nutrient pulse in the low complexity pond, but not in the intermediate complexity pond until a few days after the second nutrient pulse. The response times of chlorophyll-*a* in both the low and intermediate complexity ponds to the first nutrient pulse were similar, though the intermediate complexity pond had a longer recovery time (Table 2). Following the second nutrient pulse, Z-scores for chlorophyll-*a* concentration again significantly responded in the low and intermediate complexity ponds (Figure 4A – C). However, the low complexity pond responded 16 days faster to the second nutrient pulse and took 17 days longer to recover whereas the intermediate complexity pond had a similar response time to the first nutrient pulse, but it did not recover before the experiment was terminated (although the Z-score was trending towards recovery; Table 2).

Table 2. Response (z-score > 2) and recovery (z-score returns to <0.5) times following the nutrient pulse. If a response did not occur, it was listed as not detected (n.d.), and recovery was not recorded. Days to response is the time elapsed from the nutrient pulse whereas days to recover is the time since the response.

		Chlorophyll-*a*		Gross Primary Production		Respiration	
	Nutrient Pulse	***Days to Respond***	***Days to Recover***	***Days to Respond***	***Days to Recover***	***Days to Respond***	***Days to Recover***
Low complexity	Pulse 1	24	5	n.d.	--	n.d.	--
	Pulse 2	8	22	n.d.	--	n.d.	--
Intermediate complexity	Pulse 1	18	23	11	11	n.d.	--
	Pulse 2	20	n.d.	21	5	21	4
High complexity	Pulse 1	n.d.	--	n.d.	--	n.d.	--
	Pulse 2	n.d.	--	n.d.	--	n.d.	--

For GPP, there was only a significant response (Z-score>2) in the intermediate complexity pond after both nutrient pulses (Figure 4D – F), responding 11 days after the first pulse and 21 days after the second pulse. Additionally, GPP in the intermediate complexity pond recovered (Z-score<0.5) from the first and second pulses in eleven and five days, respectively (Table 2). There was a significant GPP response detected in the low complexity pond with a shorter rolling window (5-day) on DOY 185 with recovery on DOY 190 but not a longer rolling window (10-day) (Supplementary Material Figure S3 – S4; Table S4). There was no significant response of R or NEP following either nutrient pulse in most of the ponds (Figure 4G – L) except for the intermediate complexity pond where the Z-score of R exceeded the threshold 21 days after the second nutrient pulse, recovering 4 days later (Figure 4H). There was a significant response of R in the high complexity pond early in the time series, but it was before the first nutrient pulse (Figure 4L).

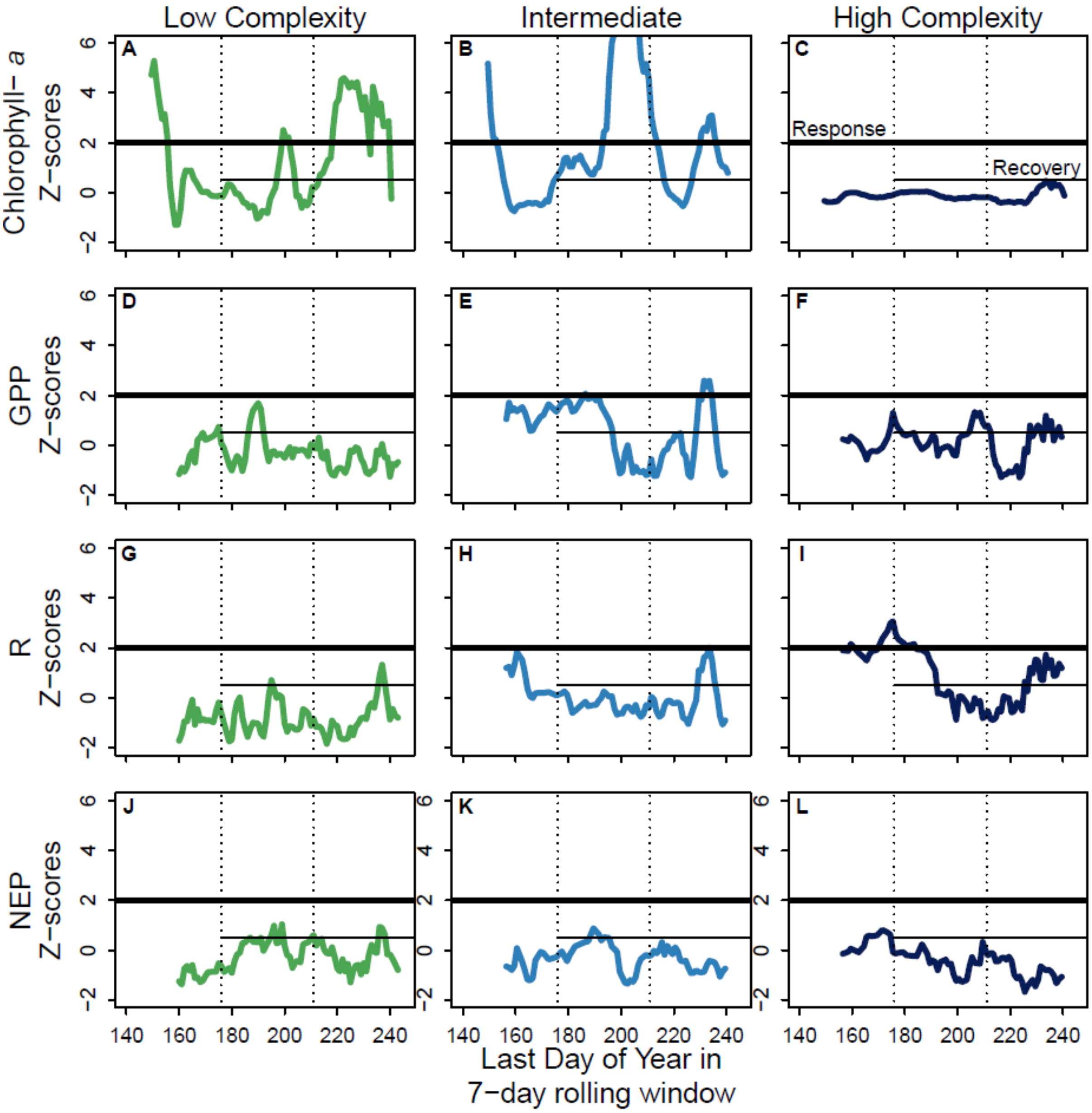

Figure 4. Time series of Z-scores of chlorophyll-*a* concentrations (A - C), gross primary production (D - F), respiration (G - I), and net ecosystem production (J - L) generated by the response detection algorithm. The thick horizontal line denotes the response threshold, and the thin horizontal line denotes the recovery threshold. The recovery threshold cannot be documented until a disturbance has occurred. The dashed vertical lines indicate the dates of the nutrient pulses.

We found mixed support for our prediction that greater complexity would reduce the chance of a critical transition following a nutrient pulse. Eigenvalues for all ponds, pulsed and reference, were purely real and lacked complex parts consistent with a saddle-node bifurcation. After the first nutrient pulse, there was only strong evidence of a critical transition in the pulsed low complexity pond where eigenvalues increased to greater than 1 on DOY 194 and again on DOY 196, 18- 20 days following the first nutrient pulse (Figure 5A). The timing of the critical transition for chlorophyll-*a* was 2-4 days prior to the peak in chlorophyll-*a* concentration (Figure 3) and 4-6 days prior to the significant response based on the response detection algorithm (Figure 4). There was no evidence of a critical transition in either the pulsed intermediate or high complexity ponds (Figure 5B – C), nor within any of the reference ponds following the first nutrient pulse (Figure 5D – F). There was no evidence of a critical transition in any of the pulsed ponds after the second nutrient pulse; however, there was evidence of a critical transition within the reference low complexity pond on DOY 232 (Figure 5D) and the reference high complexity pond on DOY 241, the last sampling day (Figure 5F).

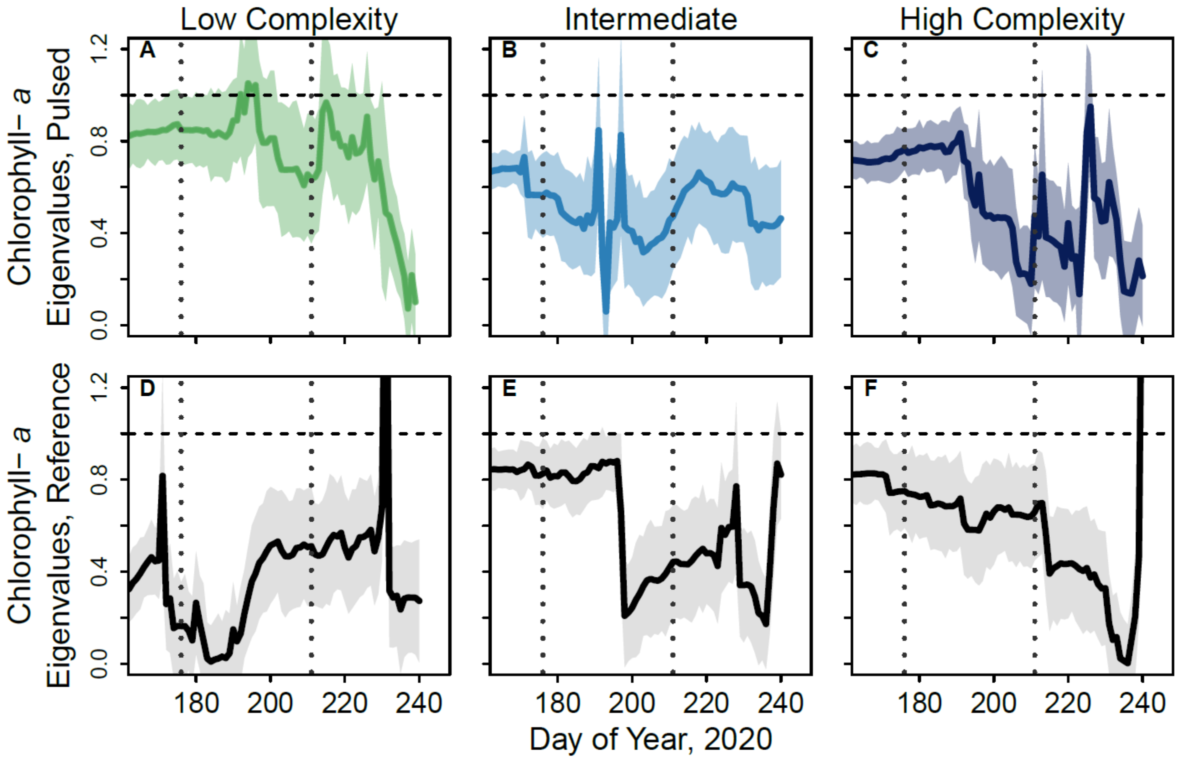

Figure 5. The eigenvalues (dark lines) and their bootstrapped standard error (shaded polygons) of chlorophyll-*a* from ponds that received nutrient pulses (A-C) and reference ponds (D-F). In all figures, the dashed vertical line denotes the nutrient pulses and the horizontal dashed line at 1 is the threshold by which eigenvalues must cross from below as evidence of a critical transition.

DISCUSSION

We established three food web structures that varied in their degree of complexity. While species richness, the number of trophic guilds, and overall fish biomass increased amongst the three food webs, the seasonal dynamics of zooplankton, periphyton, and macroinvertebrates were consistent with our expectations. First, there was stronger top-down control on planktivores in the intermediate and high complexity ponds evidenced by persistently higher zooplankton biomass especially within the high complexity pond. Second, there were regular oscillations of macroinvertebrate abundance increase and periphyton biomass decrease in the high complexity food web indicating higher prey resource use efficiency (McMeans et al. 2015). As such, though the pulsed and reference ponds lacked replication, there is evidence of predictable variable food web structure amongst the three treatments.

In support of our prediction that greater food web complexity increases resistance and resilience to disturbance, there was no response (and therefore, no recovery) of chlorophyll-*a* in the high complexity pond to nutrient pulses whereas there was a response in the low and intermediate complexity ponds. Furthermore, the low complexity pond responded swiftly after the second nutrient pulse in contrast to the intermediate complexity pond that had a similar response time to the first nutrient pulse. While there was a relatively fast recovery time in chlorophyll-*a* from the first nutrient pulse in the low complexity pond, there was a far slower recovery time following the second nutrient pulse. In similar experiments, initially fast recovery time from nutrient pulse disturbance has been observed in food webs with higher zooplanktivory (Cottingham and Schindler 2000) as we observed in the low complexity pond. Taken together, the faster response and slower recovery time in the low complexity pond after the second nutrient pulse suggests resistance and resilience to repeated nutrient pulse disturbances decreased.

The differences in response and recovery times between the intermediate and high complexity ponds also support our prediction that differences were due to stronger top-down control and greater species richness within trophic levels rather than a difference in food chain length (Ward and McCann 2017). With greater food web complexity driven by more generalist species, there was higher zooplankton biomass, macroinvertebrate density, and periphyton biomass consistent with other studies (Vadeboncoeur et al. 2005, Vander Zanden et al. 2005). Furthermore, there may have been an additional refuge effect in the high complexity ponds where the presence of predators led to altered behavior and reduced feeding rates for bluegill, yellow perch, and fathead minnows (Zanette and Clinchy 2019), strengthening top-down control on phytoplankton. It is important to note the smaller size of the ponds likely affected the realized food chain length (Post et al. 2000). However, the constrained size likely amplified differences between food web treatments, especially predator-prey interactions, generating stronger differences in response between treatments.

The dynamics of ecosystem metabolism supported our prediction that greater food web complexity would reduce the response of primary production to nutrient inputs, though the patterns were far noisier than chlorophyll-*a*. There was only a significant response in GPP following both nutrient pulses in the intermediate ponds that aligned with the peak in chlorophyll-*a* biomass observed following the first nutrient pulse. Periphyton was higher in the intermediate complexity ponds in comparison to the low complexity ponds; thus, the GPP response in this treatment also likely included periphyton (Vadeboncoeur et al. 2001). Using a smaller rolling window (5 days), GPP significantly responded in the low complexity pond following the first nutrient pulse coinciding with observed chlorophyll-*a* response at the same time. This follows the expected pattern that phytoplankton production was stimulated under reduced top-down control (Cottingham and Schindler 2000). The complex nature of stratification dynamics, floating leaf macrophytes, and dissolved oxygen changes in the bottom waters of the ponds (Albright et al. 2022), made it difficult to estimate ecosystem metabolism in these ecosystems. Nevertheless, the GPP patterns do support the chlorophyll-*a* dynamics. It is not surprising that NEP did not respond given that it is a balance of GPP and R; indeed, it had the most stable Z-scores.

It is possible the nutrient addition caused a short-lived critical transition in the low complexity pond suggesting a loss of resilience (Scheffer et al. 2015). The evidence of a critical transition in the low complexity pond following the first nutrient pulse (but not in the reference pond) suggests the chlorophyll-*a* response was due to the nutrient addition rather than stochastic environmental dynamics and that the low complexity pond had lower resilience to the nutrient pulse (Scheffer et al. 2015). Paired with the response detection algorithm results, it is likely the pulsed low complexity pond approached an elevated phytoplankton biomass stable attractor, but quickly transitioned back to the original low phytoplankton biomass attractor, as can be the case for a saddle-node bifurcation (Scheffer et al. 2015). If the critical transition was a Hopf bifurcation the eigenvalues would have had complex parts which was not the case here (Fussmann et al. 2000; Rall et al. 2008). There was no evidence of a critical transition following the second nutrient pulse in any of the pulsed ponds, though there was evidence of a critical transition in the reference low and high complexity ponds. This, however, was likely due to seasonal changes driven by the erosion of stratification and macrophyte senescence (Albright et al. 2022).

Within the experimental ponds, there were several factors outside our control that produced uncertainty. The remnant bigmouth buffalo in the pulsed low complexity pond likely contributed to the lower zooplankton biomass in that pond compared to the reference. It is also possible bigmouth buffalo contributed to the chlorophyll-*a* response in the low complexity pond and possible critical transition. However, bigmouth buffalo mainly consume copepods and large-bodied cladocerans; thus, it is unlikely that their presence broadly affected the food web structure as they are not generalist consumers (Starostka and Applegate 1970; Adámek et al. 2003). All ponds, however, were subject to increased zooplanktivory from larval bluegill and largemouth bass spawned during the study period yet both the reference and pulsed low complexity ponds had consistent zooplankton biomass dynamics. The experiment underwent two unanticipated extreme weather events: a six-day period of elevated temperatures after the first pulse and a derecho following the second pulse (Supplementary Material Figure S5). The combination of nutrients and elevated temperatures may have stimulated phytoplankton production, contributing to the strong response. The derecho on DOY 223 fully and violently mixed the water column (Albright et al. 2022), but the effect was short lived. This process may have resulted in the small increase in phytoplankton, GPP, and R in all ponds near the end of the experiment, though this signal was more likely due to divergent ecosystem trajectories from autumnal mixing and macrophyte senescence. Even so, the increase in primary production was not significant.

Greater food web complexity is increasingly recognized as an important component of food web structure in aquatic ecosystems (Rooney and McCann 2012; McMeans et al. 2016; Gutgesell et al. 2022). Here, we demonstrated empirically that even in highly spatially constrained ecosystems, a higher degree of complexity driven by increased generalist predators generating increased omnivory resulted in increased resistance and resilience of phytoplankton to nutrient pulses. Our study provides empirical and mechanistic evidence that increasing the number of generalist species could be a target for lake management to increase phytoplankton resilience to nutrients. Focusing on maintaining or enhancing food web complexity could be a long-term strategy to increase resistance and resilience to disturbances rather than focusing on removal programs that target planktivorous and benthivorous fishes (Søndergaard et al. 2008). This study provides empirical support that biodiversity and the architecture of species interactions within a food web is a key ecosystem property that makes influences resistant and resilient disturbance.

Acknowledgements: We thank Michael Tarnow, Mathew Kremer, Elena Sandry, Quin Shingai, Ellen Albright, Sofia Ferrer, Kayleigh Winston, Martin Simonson Cal Buelo, Jonathan Walter for assistance with data collection and analysis. This research was supported by the Iowa Water Center's Graduate Student Supplemental Research Competition. Butts was supported by the National Science Foundation Graduate Research Fellowship Program (DGE-1747503) and Wilkinson was supported by NSF # 2200391. Figure 1 silhouettes: Carlos Cano-Barbacil (largemouth bass), Timothy Bartley (yellow perch; fathead minnow, CC BY-SA 3.0), Corrine Avidan (bluegill), T. Michael Keesey (*Daphnia)*, Joanna Wolfe (Calanoida), Noun Project (periphyton; phytoplankton).

REFERENCES

Adámek, Z., I. Sukop, P. M. Rendón, and J. Kouřil. 2003. Food competition between 2+ tench (Tinca tinca L.), common carp (Cyprinus carpio L.) and bigmouth buffalo (Ictiobus cyprinellus Val.) in pond polyculture. Journal of Applied Ichthyology 19: 165–169.

Adje, G., L. A. Wojcik, and U. Gaedke. 2023. Functional diversity increases the resistance of a tritrophic food web to environmental changes. Theor Ecol 16: 131–150. doi:10.1007/s12080-023-00558-0

Albright, E. A., R. Ladwig, and G. M. Wilkinson. 2022. Macrophyte-hydrodynamic interactions mediate stratification and dissolved oxygen dynamics in ponds. *EarthArXiv.* https://doi.org/10.31223/X51M19

Carey, M. P., and D. H. Wahl. 2010. Interactions of multiple predators with different foraging modes in an aquatic food web. Oecologia 162: 443–452. doi:10.1007/s00442-009-1461-3

Carlander, K. 1977. Biomass, Production, and Yields of Walleye (Stizostedion vitreum vitreum) and Yellow Perch (Perca flavescens) in North American Lakes. Journal of Fisheries Research Board of Canada 34: 1602–1612.

Carmichael, W. W., and G. L. Boyer. 2016. Health impacts from cyanobacteria harmful algae blooms: Implications for the North American Great Lakes. Harmful Algae 54: 194–212. doi:10.1016/j.hal.2016.02.002

Carpenter, S. 1996. Microcosm Experiments have Limited Relevance for Community and Ecosystem Ecology. Ecology 77: 677–680.

Carpenter, S. R. 1998. The Need for Large-Scale Experiments to Assess and Predict the Response of Ecosystems to Perturbation, p. 287–312. *In* M.L. Pace and P.M. Groffman [eds.], Successes, Limitations, and Frontiers in Ecosystem Science . Springer.

Carpenter, S. R. and others. 2001. Trophic cascades, nutrients, and lake productivity: whole lake experiments. Ecol Monogr 71: 163–186.

Carpenter, S. R., E. G. Booth, and C. J. Kucharik. 2018. Extreme precipitation and phosphorus loads from two agricultural watersheds. Limnol Oceanogr 63: 1221–1233. doi:10.1002/lno.10767

Ceulemans, R., U. Gaedke, T. Klauschies, and C. Guill. 2019. The effects of functional diversity on biomass production, variability, and resilience of ecosystem functions in a tritrophic system. Sci Rep 9. doi:10.1038/s41598-019-43974-1

Cottingham, K., and D. Schindler. 2000. Effects of grazers community structure on phytoplankton response to nutrient pulses. Ecology 81: 183–200.

Dakos, V., E. H. Van Nes, P. D'Odorico, and M. Scheffer. 2012. Robustness of variance and autocorrelation as indicators of critical slowing down. Ecology 93: 264–271. doi:10.1890/11-0889.1

Duffy, J. E., B. J. Cardinale, K. E. France, P. B. McIntyre, E. Thébault, and M. Loreau. 2007. The functional role of biodiversity in ecosystems: Incorporating trophic complexity. Ecol Lett 10: 522–538. doi:10.1111/j.1461-0248.2007.01037.x

Duffy, W. G. 1998. Population dynamics, production, and prey consumption of fathead minnows (Pimephales promelas) in prairie wetlands: a bioenergetics approach. Canadian Journal of Fisheries and Aquatic Sciences 54: 15–27.

Dumont, H. J., I. Van de Velde, and S. Dumont. 1975. The dry weight estimate of biomass in a selection of Cladocera, Copepoda and Rotifera from the plankton, periphyton and benthos of continental waters. Oecologia 19: 75–97. doi:10.1007/BF00377592

Fussmann, G. F., S. P. Ellner, K. W. Shertzer, and N. G. Hairston. 2000. Crossing the Hopf Bifurcation in a Live Predator-Prey System. Science (1979) 290: 1358–360.

Griffen, B. D. 2006. Detecting emergent effects of multiple predator species. Oecologia 148: 702–709. doi:10.1007/s00442-006-0414-3

Gutgesell, M. K. and others. 2022. On the Dynamic Nature of Omnivory in a Changing World. Bioscience 72: 416–430. doi:10.1093/biosci/biab144

Guttal, V., and C. Jayaprakash. 2008. Changing skewness: An early warning signal of regime shifts in ecosystems. Ecol Lett 11: 450–460. doi:10.1111/j.1461-0248.2008.01160.x

Guy, C. S., and D. W. Willis. 1990. Structural Relationships of Largemouth Bass and Bluegill Populations in South Dakota Ponds. N Am J Fish Manag 10: 338–343. doi:10.1577/1548-8675(1990)010<0338:srolba>2.3.co;2

Ho, J. C., and A. M. Michalak. 2020. Exploring temperature and precipitation impacts on harmful algal blooms across continental U.S. lakes. Limnol Oceanogr 65: 992–1009. doi:10.1002/lno.11365

Hodgson, J. Y., and J. R. Hodgson. 2000. Exploring optimal foraging by largemouth bass (Micropterus salmoides) from three experimental lakes. Verhandlungen des Internationalen Verein Limnologie 27: 1–6.

Hurvich, C. M., and C. -L Tsai. 1993. A Corrected Akaike Information Criterion for Vector Autoregressive Model Selection. J Time Ser Anal 14: 271–279. doi:10.1111/j.1467-9892.1993.tb00144.x

Hughes, T. P. and others. 2018. Global warming transforms coral reef assemblages. Nature 556: 492–496. doi:10.1038/s41586-018-0041-2

Jackson, J., V. Resh, D. Batzer, R. Merritt, and K. Cummins. 2019. Sampling Aquatic Insects: Collection Devices, Statistical Considerations, and Rearing Procedures, p. 17–42. *In* R. Merritt, K. Cummins, and M. Berg [eds.], An Introduction to the Aquatic Insects of North America. Kendall Hunt Publishing Company.

Joosse, P. J., and D. B. Baker. 2011. Context for re-evaluating agricultural source phosphorus loadings to the great lakes. Can J Soil Sci 91: 317–327. doi:10.4141/cjss10005

Lürling, M., M. M. Mello, F. van Oosterhout, L. de S. Domis, and M. M. Marinho. 2018. Response of natural cyanobacteria and algae assemblages to a nutrient pulse and elevated temperature. Front Microbiol 9: 1–14. doi:10.3389/fmicb.2018.01851

McCauley, E. 1984. The estimation of the abundance and biomass of zooplankton in samples, p. 228–265. *In* J. Downing and F. Rigler [eds.], A manual on methods for the assessment of secondary productivity in fresh waters. Blackwell Publishing Ltd.

McMeans, B. C., K. S. McCann, M. Humphries, N. Rooney, and A. T. Fisk. 2015. Food Web Structure in Temporally-Forced Ecosystems. Trends Ecol Evol 30: 662–672. doi:10.1016/j.tree.2015.09.001

McMeans, B. C., K. S. McCann, T. D. Tunney, A. T. Fisk, A. M. Muir, N. Lester, B. Shuter, and N. Rooney. 2016. The adaptive capacity of lake food webs: From individuals to ecosystems. Ecol Monogr 86: 4–19. doi:10.1890/15-0288.1

Pace, M. L., J. J. Cole, S. R. Carpenter, and J. F. Kitchell. 1999. Trophic cascades revealed in diverse ecosystems. Trends Ecol Evol 14: 483–488. doi:10.1016/S0169-5347(99)01723-1

Polazzo, F., M. Hermann, M. Crettaz-Minaglia, and A. Rico. 2023. Impacts of extreme climatic events on trophic network complexity and multidimensional stability. Ecology 104. doi:10.1002/ecy.3951

Pomeranz, J. P. F., J. C. Finlay, and A. Terui. 2023. Ecosystem size and complexity as extrinsic drivers of food chain length in branching ecosystems. Ecosphere 14. doi:10.1002/ecs2.4648

Post, D., M. Pace, and N. Hairston Jr. 2000. Ecosystem size determines food-chain length in lakes. Nature 405: 1047–1049.

Prein, A. F., C. Liu, K. Ikeda, S. B. Trier, R. M. Rasmussen, G. J. Holland, and M. P. Clark. 2017. Increased rainfall volume from future convective storms in the US. Nat Clim Chang 7: 880–884. doi:10.1038/s41558-017-0007-7

R Core Team. 2022. R: A language and environment for statistical computing.

Rall, B. C., C. Guill, and U. Brose. 2008. Food-web connectance and predator interference dampen the paradox of enrichment. Oikos 117: 202–213. doi:10.1111/j.2007.0030-1299.15491.x

Rooney, N., and K. S. McCann. 2012. Integrating food web diversity, structure and stability. Trends Ecol Evol 27: 40–46. doi:10.1016/j.tree.2011.09.001

Rose, K. C., L. A. Winslow, J. S. Read, E. K. Read, C. T. Solomon, R. Adrian, and P. C. Hanson. 2014. Improving the precision of lake ecosystem metabolism estimates by identifying predictors of model uncertainty. Limnol Oceanogr Methods 12: 303–312. doi:10.4319/lom.2014.12.303

Scheffer, M., S. R. Carpenter, V. Dakos, and E. H. Van Nes. 2015. Generic Indicators of Ecological Resilience: Inferring the Chance of a Critical Transition. Annu Rev Ecol Evol Syst 46: 145–167. doi:10.1146/annurev-ecolsys-112414-054242

Schindler, D. W. 1998. Replication versus realism: The need for ecosystem-scale experiments. Ecosystems 1: 323–334. doi:10.1007/s100219900026

Seneviratne, S. and others. 2021. Weather and Climate Extreme Events in a Changing Climate, p. 1513–1766. *In* V. Masson-Delmotte et al. [eds.], Climate Change 2021: The Physical Science Basis. Contribution of Working Group I to the Sixth Assessment Report of the Intergovernmental Panel on Climate Change. Cambridge University Press.

Søndergaard, M., L. Liboriussen, A. R. Pedersen, and E. Jeppesen. 2008. Lake restoration by fish removal: Short- and long-term effects in 36 Danish lakes. Ecosystems 11: 1291–1305. doi:10.1007/s10021-008-9193-5

Starostka, V. J., and R. L. Applegate. 1970. Food Selectivity of Bigmouth Buffalo , Ictiobus cyprinellus , in Lake Poinsett , South Dakota. Trans Am Fish Soc 99: 571–576. doi:10.1577/1548-8659(1970)99<571

Stockwell, J. D. and others. 2020. Storm impacts on phytoplankton community dynamics in lakes. Glob Chang Biol 1–27. doi:10.1111/gcb.15033

Taranu, Z. E., S. R. Carpenter, V. Frossard, J. P. Jenny, Z. Thomas, J. C. Vermaire, and M. E. Perga. 2018. Can we detect ecosystem critical transitions and signals of changing resilience from paleo-ecological records? Ecosphere 9. doi:10.1002/ecs2.2438

Turner, M. G. and others. 2020. Climate change, ecosystems and abrupt change: Science priorities. Philosophical Transactions of the Royal Society B: Biological Sciences 375. doi:10.1098/rstb.2019.0105

Tyson, J. T., and R. L. Knight. 2001. Response of Yellow Perch to Changes in the Benthic Invertebrate Community of Western Lake Erie. Trans Am Fish Soc 130: 766–782.

Vadeboncoeur, Y., D. Lodge, and S. Carpenter. 2001. WHOLE-LAKE FERTILIZATION EFFECTS ON DISTRIBUTION OF PRIMARY PRODUCTION BETWEEN BENTHIC AND PELAGIC HABITATS. Ecology 82: 1065–1077.

Vadeboncoeur, Y., K. S. McCann, M. J. Vander Zanden, and J. B. Rasmussen. 2005. Effects of multi-chain omnivory on the strength of trophic control in lakes. Ecosystems 8: 682–693. doi:10.1007/s10021-003-0149-5

Vanni, M. J., W. H. Renwick, J. L. Headworth, J. D. Auch, and M. H. Schaus. 2001. Dissolved and particulate nutrient flux from three adjacent agricultural watersheds: A five-year study. Biogeochemistry 54: 85–114. doi:10.1023/A:1010681229460

Walter, J. A., C. D. Buelo, A. F. Besterman, S. J. Tassone, J. W. Atkins, and M. L. Pace. 2022. An algorithm for detecting and quantifying disturbance and recovery in high-frequency time series. Limnol Oceanogr Methods 20: 338–349. doi:10.1002/lom3.10490

Walter, J., and C. Buelo. 2022. jonathan-walter/disturbhf: lno-methods paper version (v1.0.0).doi:https://doi.org/10.5281/zenodo.6472546

Ward, C. L., and K. S. McCann. 2017. A mechanistic theory for aquatic food chain length. Nat Commun 8: 2028. doi:10.1038/s41467-017-02157-0

Ward, C. L., K. S. Mccann, and N. Rooney. 2015. HSS revisited: Multi-channel processes mediate trophic control across a productivity gradient. Ecol Lett 18: 1190–1197. doi:10.1111/ele.12498

Werner, E. E., and D. J. Hall. 1988. Ontogenetic habitat shifts in bluegill: the foraging rate-predation risk trade-off. Ecology 69: 1352–1366. doi:10.2307/1941633

Winslow, L. A., J. A. Zwart, R. D. Batt, H. A. Dugan, R. I. Woolway, J. R. Corman, P. C. Hanson, and J. S. Read. 2016. LakeMetabolizer: an R package for estimating lake metabolism from free-water oxygen using diverse statistical models. Inland Waters 6: 622–636. doi:10.1080/iw-6.4.883

Wojcik, L. A., R. Ceulemans, and U. Gaedke. 2021. Functional diversity buffers the effects of a pulse perturbation on the dynamics of tritrophic food webs. Ecol Evol 11: 15639–15663. doi:10.1002/ece3.8214

Wootton, K. L., and D. B. Stouffer. 2016. Species' traits and food- web complexity interactively affect a food web ' s response to press disturbance. Ecosphere 7: 1–13.

Vander Zanden, M. J., T. E. Essington, and Y. Vadeboncoeur. 2005. Is pelagic top-down control in lakes augmented by benthic energy pathways? Canadian Journal of Fisheries and Aquatic Sciences 62: 1422–1431. doi:10.1139/f05-042

Zanette, L. Y., and M. Clinchy. 2019. Ecology of fear. Current Biology 29: R309–R313. doi:10.1016/j.cub.2019.02.042

Zscheischler, J. and others. 2018. Future climate risk from compound events. Nat Clim Chang 8: 469–477. doi:10.1038/s41558-018-0156-3

Data Availability Statement: Data will be archived through the Environmental Data Initiative and given a unique digital object identifier. Scripts and data for analysis and figure generation are available at https://github.com/tjbutts/hort-benthic-pelagic and will be archived through Zenodo upon acceptance.

Conflict of Interest: The authors declare no conflict of interest

Food web complexity alters phytoplankton resistance and resilience to nutrient pulses in experimental ecosystems

Tyler J. Butts[1,2*], Robert A. Johnson[1,3], Michael J. Weber[4], Grace M. Wilkinson[1,2,3]

[1]Department of Ecology, Evolution, and Organismal Biology, Iowa State University, Ames, IA, USA
[2]Present Address: Center for Limnology, University of Wisconsin-Madison, WI, USA
[3]Present Address: Department of Integrative Biology, University of Wisconsin-Madison, Madison, WI, USA
[4]Department of Natural Resource Ecology and Management, Iowa State University, Ames, IA, USA
* Corresponding author: tyler.james.butts@gmail.com
Tyler J. Butts: tjbutts@wisc.edu (https://orcid.org/0000-0002-3562-365X)
Robert A. Johnson: robert.a.johnson@wisc.edu (https://orcid.org/0000-0003-4072-5623)
Michael J. Weber: mjw@iastate.edu (https://orcid.org/0000-0003-0430-3087)
Grace M. Wilkinson: gwilkinson@wisc.edu (https://orcid.org/0000-0003-4051-2249)

Supplementary Material

Methods

Periphyton

For periphyton, a modified Hester-Dendy sampler (173.28 cm^2) was deployed for two-week periods in each pond and areal chlorophyll-*a* was measured based on analysis of the biomass that grew on the artificial substrate during the deployment. Periphyton was brushed, scraped, and rinsed off the substrate (0.017 m^2) with deionized water and diluted to a known volume in amber bottles before analysis (Jacoby et al. 1991; Carey and Wahl 2011). Samples from each pond were homogenized to loosen algal 'clumps' and filtered onto Whatman glass fiber filters (0.45 μm). Areal chlorophyll-*a* (μg/m^2) was measured via acetone extraction (Standard Methods 10200-H) using sonication (Bidigare et al. 2005) and analyzed using fluorometry (EPA Method 445.0) on a Turner Designs Trilogy Fluorometer (Arar and Collins 1997; Childress et al. 1999; Turner Designs 2001).

Nutrients

Phosphorus (total phosphorus, soluble reactive phosphorus) was measured via the phosphomolybdenum blue method (EPA method 365.1 v2) and nitrogen (total nitrogen, nitrate and nitrite, ammonium) was measured via second-derivative ultraviolet spectroscopy(Crumpton et al. 1992; Childress et al. 1999) using an HP 8435 Spectrophotometer. Total phosphorus and nitrogen samples underwent a persulfate digestion before analysis to transform all P- or N-containing compounds into dissolved forms.

Zooplankton

Zooplankton were identified using a Leica MZ8 stereomicroscope connected to Motic Images software in a 1 mL subsample. If less than 60 organisms were identified within the 1 mL subsample, another subsample was counted. Up to 25 individuals per taxon were measured per sample to calculate dry mass per liter using standard length-mass regressions (Dumont et al. 1975; McCauley 1984).

Macroinvertebrates

Macroinvertebrates were sampled using a stovepipe sampler that had a diameter of 0.3 m. To assist with identification, we added 0.1% Rose Bengal Dye to preserved macroinvertebrate samples. In the lab, macroinvertebrates were further sieved on a 500-µm pan sieve and individuals were removed and identified to the lowest possible order or family. A stereomicroscope was used to identify mollusks and insects to family. Leeches and oligochaetes were identified to class. This level of taxonomic resolution is sufficient to reflect community patterns (Bowman and Bailey 1997). Sorted individuals were then used to calculate taxon richness and density (number of individuals/m^2).

Dissolved Oxygen Data Cleaning

Dissolved oxygen (DO) concentration was measured every 30 minutes in the surface waters of each pond over the course of the 96-day experiment. The sensor was lowered slowly at a rate of 1 m per 15 s through the water column, continuously logging chlorophyll-*a* concentration. Prior to calculating daily rates of ecosystem metabolism, DO data were inspected and cleaned to account for times when a change in DO concentration was likely a result of physical processes (e.g., vertical mixing) rather than biological production or respiration. We used a conservative threshold of a change of 2.0 mg DO L^{-1} to identify these times. All times when DO concentration decreased by 2.0 mg L^{-1} or more from the previous measurement (i.e., a 2.0 mg L^{-1} drop in 30 minutes) were flagged and removed along with the subsequent five measurements (three hours total). These three-hour periods were then backfilled via linear interpolation. The majority of days did not require any cleaning and backfilling of DO data. Out of 576 total days (96 per pond), 345 days did not have any flagged DO measurements (60%), 144 days had one flagged measurement (25%), 71 days had two flagged measurements (12.2%), and only 16 days had three or more flagged measurements (2.8%).

As described in the manuscript text, calculating daily rates of metabolism using the free-oxygen method can result in erroneous estimates (i.e., negative GPP, positive R), and any days for which calculations returned an erroneous estimate were removed prior to further analyses. This resulted in the removal of 62 days due to erroneous metabolism estimates (range 4 – 18 days across all ponds), 40 of which were from days that did not have any flagged and cleaned DO measurements.

SUPPLEMENTARY TABLES

Table S1. Mass, in grams, of nitrogen and phosphorus added to the experimental research ponds for each nutrient pulse along with the percent increase in ambient phosphorus concentrations.

	NH_4NO_3	$NaH_2PO_4(H_2O)_2$	Ambient increase
Nutrient Pulse 1	21.36	3.33	3 %
Nutrient Pulse 2	45.01	7.02	5 %

Table S2. Akaike Information Criterion corrected for small sample size (AICc) of online dynamic linear autoregressive models of chlorophyll-*a* concentration for each experimental pond at optimal order (p) of 1 or 2.

	p = 1	p = 2	ΔAICc
Low Coupling – pulsed	359.38	356.51	2.87
Low Coupling – reference	426.81	457.05	30.24
Intermediate – pulsed	554.2	580.49	26.29
Intermediate – reference	321.31	327.75	6.44
High Coupling – pulsed	245.5	273.39	27.89
High Coupling – reference	401.88	403.55	1.67

Table S3. The number of individuals identified in the stomach contents of fish at the end of the experiment collected via gastric lavage grouped by taxonomic identity. Macrophytes included plant pieces and stems, miscellaneous eggs were mostly frog eggs but some fish eggs as well, and frog refers to adults. If individuals of a certain taxa were not identified, they were marked as not detected (n.d.).

		Bluegill	***Yellow Perch***	***Largemouth Bass***
Low Coupling	Zooplankton	32	6	--
	Macroinvertebrate	115	45	--
	Misc. Eggs	3	n.d.	--
	Macrophytes	16	8	--
	Larval fish	n.d.	11	--
	Frog	n.d.	n.d.	--
Intermediate	Zooplankton	11	n.d.	n.d.
	Macroinvertebrate	55	25	22
	Misc. Eggs	10	n.d.	n.d.
	Macrophytes	16	1	1
	Larval fish	n.d.	7	4
	Frog	n.d.	n.d.	n.d.
High Coupling	Zooplankton	11	2	n.d.
	Macroinvertebrate	72	35	6
	Misc. Eggs	1	--	n.d.
	Macrophytes	15	2	1
	Minnow	n.d.	2	1
	Larval fish	n.d.	n.d.	n.d.
	Frog	n.d.	n.d.	1

Table S4. Response detection algorithm results for chlorophyll-*a*, gross primary production, respiration, and net ecosystem production with three rolling window lengths: five days, seven days, and ten days. The days to respond quantifies the number of days following the first or second nutrient pulse that it took Z-scores to move above the response threshold (Z = 2.0). Days to recover quantifies the number of days, once the Z-scores passed the response threshold, to move below the recovery threshold (Z = 0.5).

			Chlorophyll-*a*		Gross Primary Production		Respiration	
	Window	***Nutrient Pulse***	***Days to Respond***	***Days to Recover***	***Days to Respond***	***Days to Recover***	***Days to Respond***	***Days to Recover***
Low Coupling	7 days	Pulse 1	24	5	n.d.	--	n.d.	--
	7 days	Pulse 2	8	22	n.d.	--	n.d.	--
Intermediate Coupling	7 days	Pulse 1	18	23	11	11	n.d.	--
	7 days	Pulse 2	20	n.d.	21	5	21	4
High Coupling	7 days	Pulse 1	n.d.	--	n.d.	--	n.d.	--
	7 days	Pulse 2	n.d.	--	n.d.	--	n.d.	--
Low Coupling	5 days	Pulse 1	24	4	9	5	n.d.	--
	5 days	Pulse 2	8	14	n.d.	--	n.d.	--
Intermediate Coupling	5 days	Pulse 1	18	22	18	22	n.d.	--
	5 days	Pulse 2	19	9	19	9	21	4
High Coupling	5 days	Pulse 1	n.d.	--	n.d.	--	n.d.	--
	5 days	Pulse 2	n.d.	--	n.d.	--	n.d.	--
Low Coupling	10 days	Pulse 1	25	6	n.d.	--	n.d.	--
	10 days	Pulse 2	8	n.d	n.d.	--	n.d.	--
Intermediate Coupling	10 days	Pulse 1	5	38	4	17	n.d.	--
	10 days	Pulse 2	19	n.d.	22	4	n.d.	--
High Coupling	10 days	Pulse 1	n.d.	--	n.d.	--	n.d.	--
	10 days	Pulse 2	n.d.	--	n.d.	--	21	--

SUPPLEMENTAL FIGURES

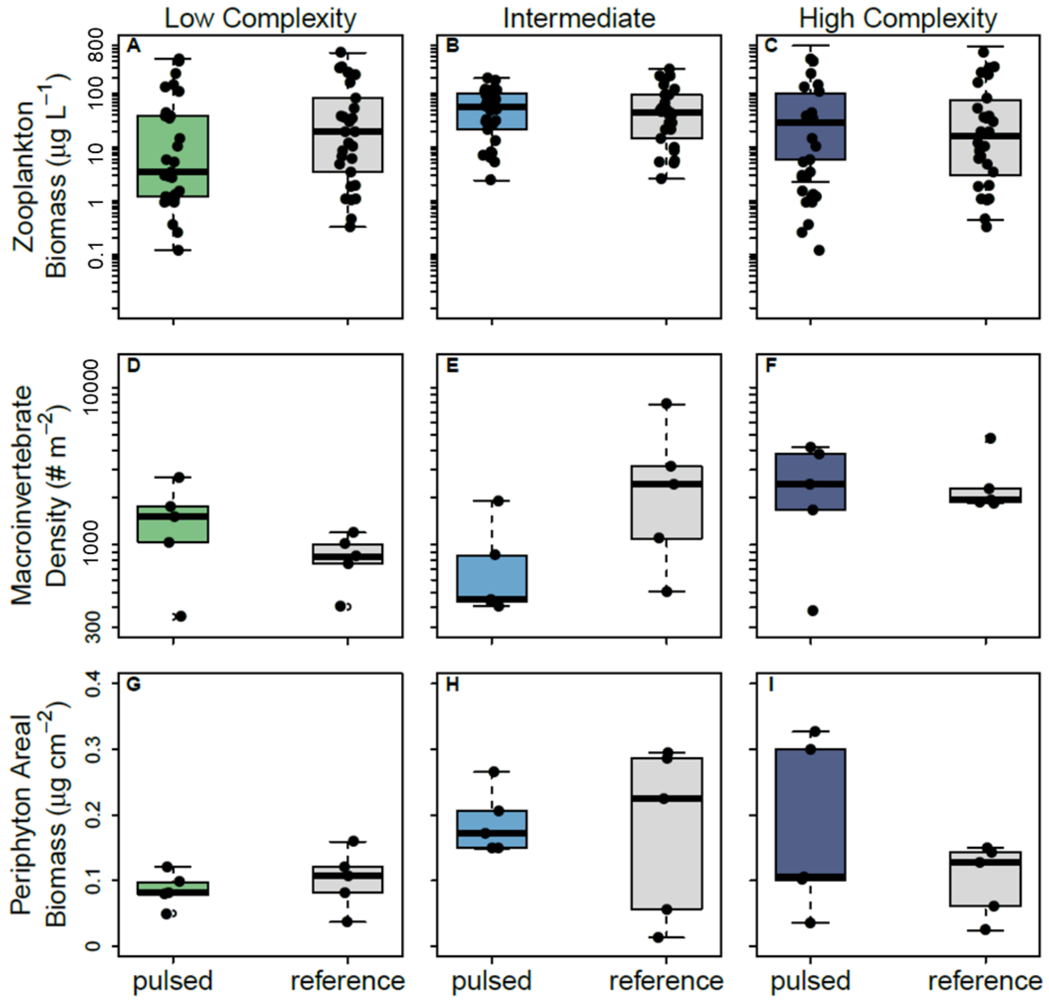

Figure S1. Food web context for experimental ponds over the course of the experiment for zooplankton biomass in micrograms per liter (µg L^{-1}; A - C), macroinvertebrate density in number per square meter (# m^{-2}; D – F), and periphyton areal biomass in micrograms per square centimeter (µg m^{-2}; G – I).

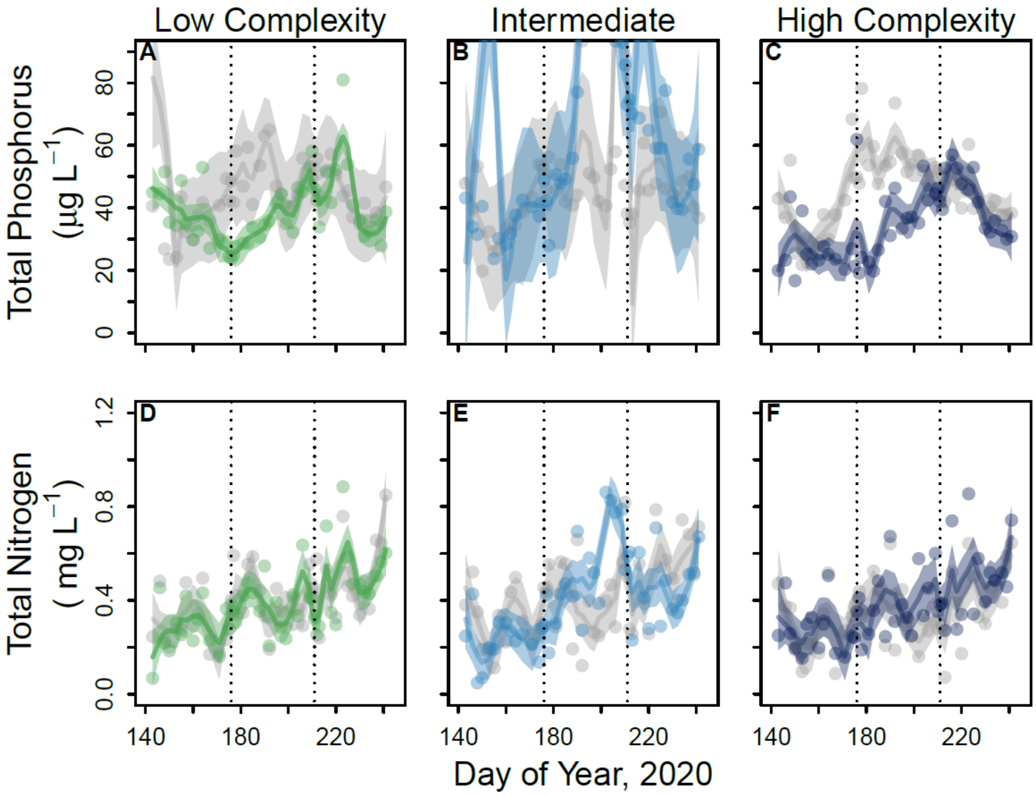

Figure S2. Time series of total nitrogen (mg L^{-1}) and phosphorus (µg L^{-1}). Data were fitted with LOESS regression analysis (20% span) for visualization purposes, error is defined by the shaded region. The dark colored line indicates the disturbed time series, and the gray line indicates the reference time series. In all figures, the dashed vertical line denotes the nutrient pulses on day of year 176 and 211.

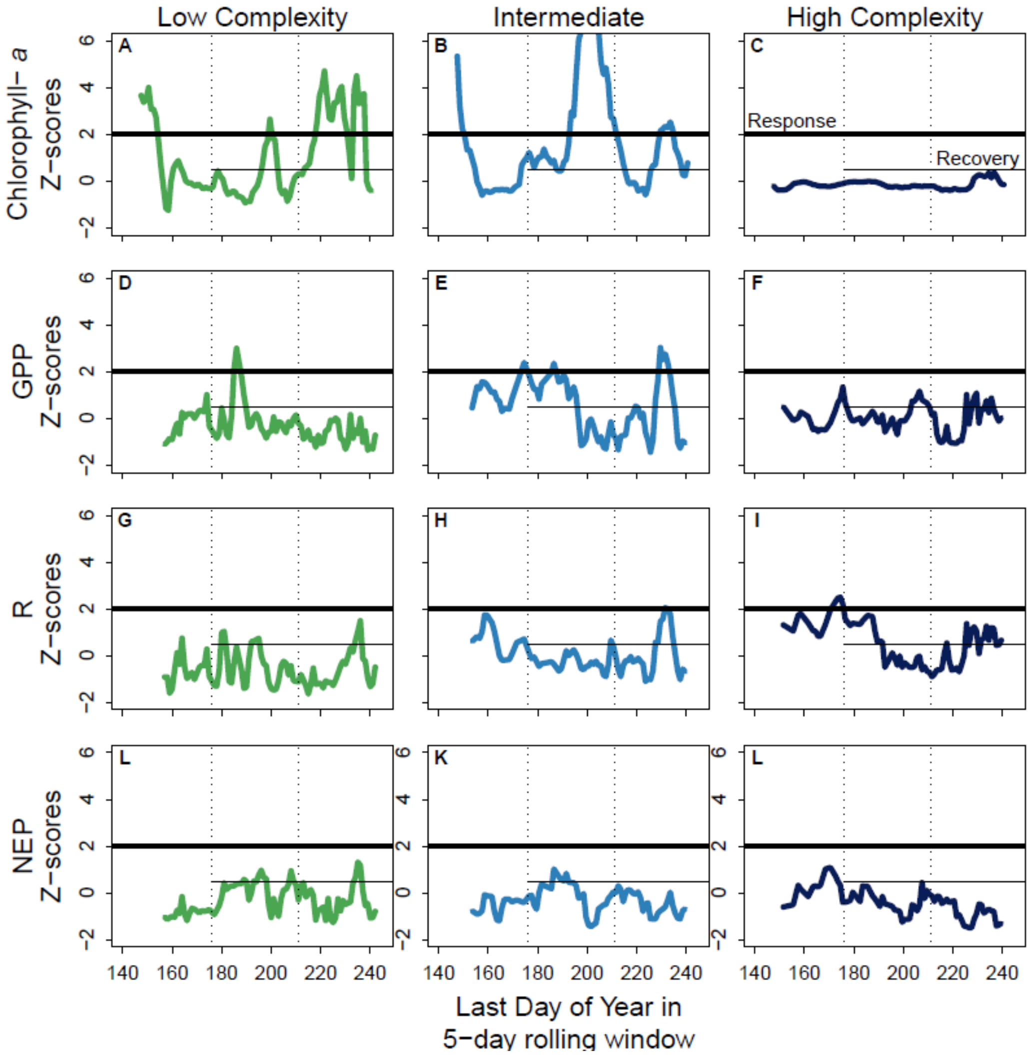

Figure S3. Time series of modified Z-scores of chlorophyll-*a* concentrations (A - C), gross primary production (D - F), respiration (G - I), and net ecosystem production (J - L) generated by the response detection algorithm (Walter et al. 2022) with a 5-day rolling window. In all figures the thick horizontal line denotes the response threshold, and the thin horizontal line denotes the recovery threshold. The recovery threshold can't be documented until a disturbance has occurred. The dashed vertical lines indicate when the nutrient pulses were delivered to each pond on day of year 176 and 211.

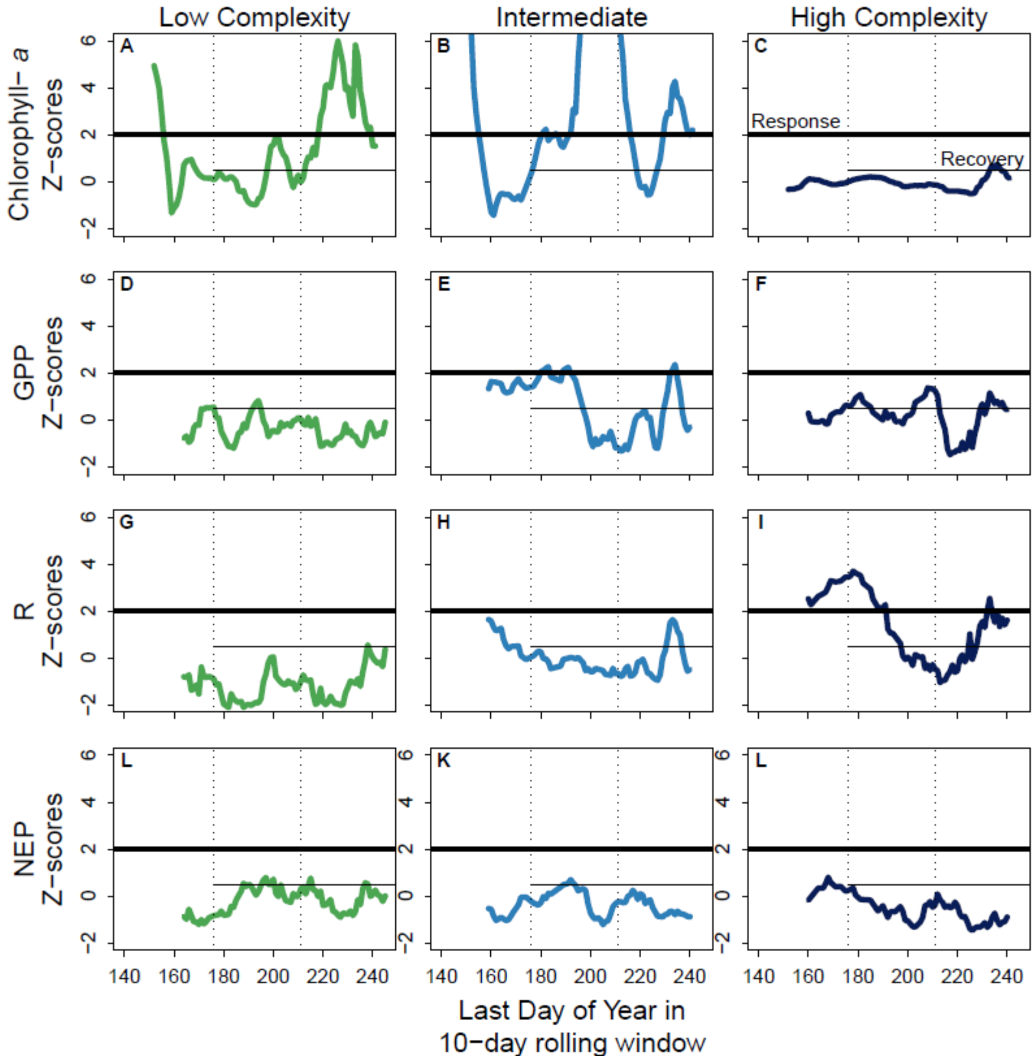

Figure S4. Time series of modified Z-scores of chlorophyll-*a* concentrations (A - C), gross primary production (D - F), respiration (G - I), and net ecosystem production (J - L) generated by the response detection algorithm (Walter et al. 2022) with a 10-day rolling window. In all figures the thick horizontal line denotes the response threshold, and the thin horizontal line denotes the recovery threshold. The recovery threshold can’t be documented until a disturbance has occurred. The dashed vertical lines indicate when the nutrient pulses were delivered to each pond on day of year 176 and 211.

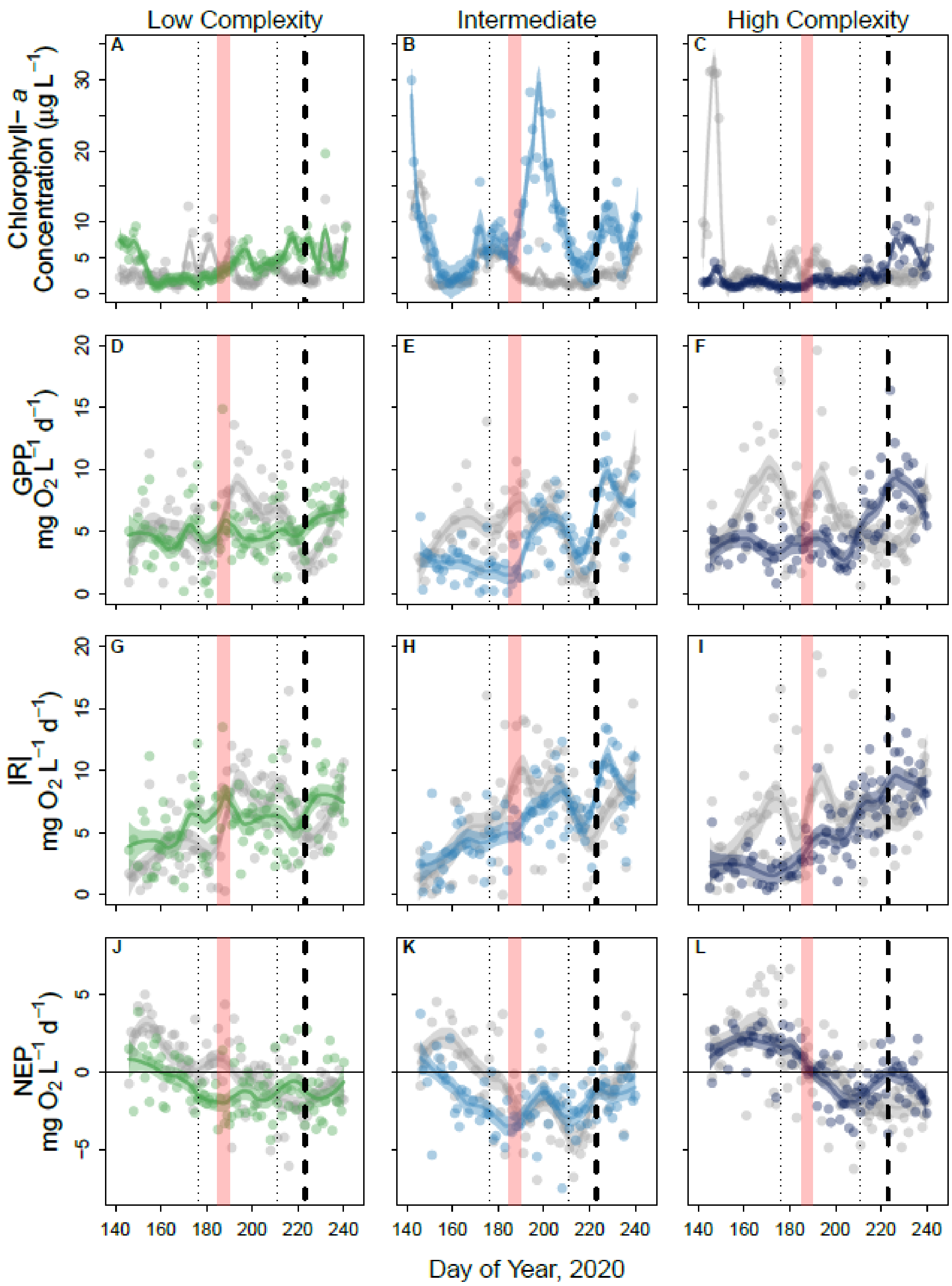

Figure S5. Dynamics of chlorophyll-*a* in micrograms per liter (µg L^{-1}), gross primary production (GPP), respiration (absolute value, |R|), and net ecosystem production (NEP) in milligrams of oxygen per liter per day (mg O_2 L^{-1} d^{-1}). Data were fitted with LOESS regression analysis for visualization purposes, error is defined by the shaded region. The dark colored line indicates the disturbed time series, and the gray line indicates the reference time series. In all figures, the dashed vertical line denotes the nutrient pulses on day of year 176 and 211 and the horizontal line at zero (J – L) shows whether the ecosystem was autotrophic (NEP > 0) or heterotrophic (NEP < 0). The five-day period of elevated surface water temperature is a red polygon, and the thick dashed vertical line indicates when the 2020 Iowa derecho occurred on DOY 223.

REFERENCES

Arar, E., and G. Collins. 1997. In Vitro determination of Chlorophyll a and Pheophytin a in marine and freshwater algae by fluorescence Revision 1.2.

Bowman, M. F., and R. C. Bailey. 1997. Does taxonomic resolution affect the multivariate description of the structure of freshwater benthic macroinvertebrate communities? Canadian Journal of Fisheries and Aquatic Sciences 54: 1802–1807. doi:10.1139/f97-085

Carey, M. P., and D. H. Wahl. 2011. Fish diversity as a determinant of ecosystem properties across multiple trophic levels. Oikos 120: 84–94. doi:10.1111/j.1600-0706.2010.18352.x

Childress, C., W. Foreman, B. Conner, and T. Maloney. 1999. New Reporting Procedures Based on Long-Term Method Detection Levels and Some Considerations for Interpretations of Water-Quality Data Provided by the U.S. Geological Survey National Water Quality Laboratory.

Crumpton, W., T. Isenhart, and P. Mitchell. 1992. Nitrate and Organic N Analysis using Second-Derivative Spectroscopy. Limnol Oceanogr 37: 907–913.

Dumont, H. J., I. Van de Velde, and S. Dumont. 1975. The dry weight estimate of biomass in a selection of Cladocera, Copepoda and Rotifera from the plankton, periphyton and benthos of continental waters. Oecologia 19: 75–97. doi:10.1007/BF00377592

Jacoby, J. M., D. D. Bouchard, and C. R. Patmont. 1991. Response of periphyton to nutrient enrichment in lake chelan, wa. Lake Reserv Manag 7: 33–43. doi:10.1080/07438149109354252

McCauley, E. 1984. The estimation of the abundance and biomass of zooplankton in samples, p. 228–265. *In* J. Downing and F. Rigler [eds.], A manual on methods for the assessment of secondary productivity in fresh waters. Blackwell Publishing Ltd.

Standard Methods for the Examination of Water and Wastewater. 2011. 22nd Edition. Method 10200-H.

Turner Designs. 2001. A procedure for measuring extracted Chlorophyll-*a* free from the errors associated with Chlorophyll-*b* and pheopigments. http//www.turnerdesigns.com/t2/doc/appnotes/998_9000.html